

# Vortex and ULF wave structures in the plasma sheet of the Earth magnetosphere

*D. A. Saliuk<sup>1\*</sup>; O. V. Agapitov<sup>1,2</sup>*

<sup>1</sup>Taras Shevchenko National University of Kyiv, Glushkova ave., 4, 03127, Kyiv, Ukraine

<sup>2</sup>LPC2E/CNRS, University of Orleans, France

We studied the ULF wave packet propagation in the Earth plasma sheet making use of the magnetic field measurements from FGM detector and plasma properties from CORRAL detector aboard the Interball-Tail spacecraft. The MHD vortex structures were observed simultaneously with the Pc5 ULF waves. The vortex spatial scale was found to be about 1200–3600 km and the velocity is 4–16 km/s transverse to the background magnetic field. We studied numerically the dynamics of the initial vortex perturbations in the plasma system with parameters observed in the Earth plasma sheet. The system with the vector nonlinearity was processed making use of the full reduction scheme. The good agreement of the experimental value of the vortex structure velocity with numerical results was obtained. The velocity was found to be close to the local plasma drift velocity.

**Key words:** MHD waves and instabilities, plasma waves and instabilities, nonlinear phenomena

## INTRODUCTION

Vortex structures are common in the near-Earth space. The large scale (much greater than ion gyroradius) MHD vortices were detected in the Earth plasma sheet and magnetosphere tail by ISEE-1,2 [7, 11, 12, 13, 20], by THEMIS [14, 21], by Cluster [25] in the low-latitude boundary layers by GEOTAIL [9], and in the magnetospheres of Saturn on the basis of Cassini observations [16]. Those results were interpreted as an evidence for a convective vortex street induced by the Kelvin-Helmholtz instability as a nonlinear phase of surface wave growth [5]. Spacecraft measurements showed that the night magnetosphere vortex modes are observed very often [11]. Multi-point measurements of vortex structure were provided in the frame of the ISEE project in 1978 when the vortex plasma motion was registered by the two closely spaced spacecraft ISEE 1 and ISEE 2 [12]. The magnetometer and the plasma analyzers aboard spacecraft allowed to obtain the three-dimensional structure of the magnetic field perturbations and the plasma flow velocity with high time resolution. During 19 months of ISEE 1 and ISEE 2 observations 169 vortex events were detected [12]. Vortices were observed mainly in the morning sector ( $Y_{GSM} < 0$ ). The magnetic field and the plasma flow velocity vector rotated in phase. In a single structure a complete rotation of magnetic field and velocity vector had the period of 5-20 minutes. There

was no clear correlation between the period of rotation and the distance from the magnetopause. The lifetime was usually found to be several full rotations. The events were observed almost identically aboard ISEE 1 and ISEE 2, which had spatial separation more than 1000 km, i.e. several ion Larmor radii. Making use of the magnetic field vector rotation phase difference aboard ISEE 1 and ISEE 2 the spatial scale of vortex structures was estimated to be 1–10  $R_E$ , and the phase velocity about 100 km/s. On the other hand, a much smaller spatial scale of the structure (about 5000 km) from the anisotropy of energetic particle flux was obtained in [20]. In [20] it was shown that the analysis of the phase shift yields only the upper limit value of the spatial scale and in general the results from the magnetic field were consistent with results obtained from particle flux analysis. The spatial scale can vary from 5000 km for the inner magnetosphere up to 7–20  $R_E$  in the distant tail [11]. Near the magnetopause vortices move tailward with velocity about 100–300 km/s that is close to the magnetosheath plasma flow velocity. This suggests the generation of these structures by boundary instability, such as Kelvin-Helmholtz instability confirmed by numerical simulations [10]. The magnetopause surface instabilities cannot explain generation of vortex in the inner magnetosphere especially with small scale (about Larmor radius). The scale sizes of the two vortices observed during moderate geomagnetic activity at the outer radiation belt and

\*dima.ubf@gmail.com

the ring current region by the Cluster fleet are about 800 km and 1100 km, respectively [25]. Alternative for generation of vortex structures is the MHD instabilities carried out by geomagnetic activity. Vortex events often were found to be accompanied by low-frequency geomagnetic activity [11]. Association of the Pc5 waves, which widely occur in the Earth magnetosphere [2, 3, 4, 5] with large-scale plasma motions were studied making use of the GEOTAIL measurements [17] and the Interball-Tail measurements in the plasma sheet ( $X_{GSE} > -15R_E$ ) and show statistically the evidence of this connection [1, 22, 23]. In [14] the full scenario of the magnetosphere vortex generation and coupling with ionosphere processes is presented on the basis of combined ground (Canadian magnetometer array) and space observations (THEMIS spacecraft).

In this paper we perform the case study of the vortex structure observed aboard Interball-Tail spacecraft simultaneously with large amplitude ULF wave packet in the Earth plasma sheet. Also the technique developed for automatic detection vortex like structures in data is presented. The observed properties of vortex structure are compared with results of numerical simulation.

## DATA DESCRIPTION

### AND PROCESSING TECHNIQUE

To study the variations of the magnetic field and plasma velocity flow we apply the correlation spectral analysis of vector variables in a form presented in [18]. For the vector variables two types of the correlation functions and corresponding Fourier spectra are provided – the vector and the scalar, which are defined as the following: for two vector variables  $\mathbf{x}(t) = \{x_1, x_2, x_3\}$  and  $\mathbf{y}(t) = \{y_1, y_2, y_3\}$  the mutual scalar spectrum is defined as the scalar product of their components Fourier spectra  $SCS(f) = \left(\frac{2}{N}\right) (\mathbf{X}^*(f), \mathbf{Y}(f))$ , where vectors  $\mathbf{X}(t) = \{X_1, X_2, X_3\}$  and  $\mathbf{Y}(t) = \{Y_1, Y_2, Y_3\}$  are complex in general, dependent on frequency.  $\mathbf{X}(f)$  and  $\mathbf{Y}(f)$  are the Fourier transformation of  $\mathbf{x}(t)$  and  $\mathbf{y}(t)$ , respectively. The complex conjugation is marked with asterisk,  $N$  is the number of measurements. Vector mutual spectrum for variables  $\mathbf{x}$  and  $\mathbf{y}$  is defined as  $VCS(f) = \left(\frac{2}{N}\right) [\mathbf{X}^*(f), \mathbf{Y}(f)]$ .

$VCS(f)$  is also the three dimensional vector variable. By analogy the scalar and vector auto-spectra are defined. The scalar auto-spectrum is the module of vector  $\mathbf{X}(f)$  and it is real and positive. This value contains the full spectral power including longitudinal, angular and rotational oscillations. Vector auto-spectrum is  $VS(f) = \left(\frac{2}{N}\right) [\mathbf{X}^*(f), \mathbf{X}(f)]$  is three-

dimensional and imaginary. The magnitude of the vector  $VS(f)$  includes only the rotation (elliptically polarized variations) of  $\mathbf{x}$ . Linearly polarized oscillations, as well as angular oscillations do not contribute to the  $VS(f)$ . To determine the time intervals of vortex activity we study the scalar and vector auto-spectrum of the magnetic field and plasma flow velocity variations. In the presented paper we detect the vortex structures using the ratio  $VS(f)/|\mathbf{X}(f)|$ . This ratio is less than unity and determines contribution of the rotational oscillations to the full spectral power.

We use for presented study the magnetic field measurements by MIF-M [15] and plasma parameters from the plasma analyzer instrument CORALL [24]. The Interball-Tail during the intervals of time considered in this study was in the plasma distant sheet: distance from the Earth  $\sim 20R_E$  and MLT 3:30.

## VORTEX STRUCTURES

### IN THE PLASMA SHEET

The periodic process with temporal localization has been detected aboard Interball-Tail on October 23, 1995. Fig.1 shows the magnetic field absolute value dynamics detected aboard Interball-Tail around the processed time interval. The vector structure is observed during high amplitude ULF waves detected both in the magnetic field and in the plasma density perturbations. The magnetic field perturbations have component parallel to the background magnetic field. The magnetic field pressure oscillations are observed with  $180^\circ$  phase shift with plasma pressure perturbations. This is usual for slow magnetosonic waves [3]. The frequency range and amplitude temporal behaviour are usual for Ps6 wave packets observed as a rule in the magnetosphere tail and associated with substorm onsets [8]. The interval of interest was exactly during intermediate geomagnetic storm (minimal Dst  $\sim -105$ ) recovery phase of substorm event (AE index  $\sim 1500$  nT) thus the observed magnetic field perturbation can be directly connected to the tail magnetic field structure changes. The dynamics of perturbation from magnetic field measurements provided by CANOPUS magnetometer stations is shown in Fig. 1. The real part of wavelet transform (Morlet) indicates well the localized in time periodic process with frequency  $\sim 2$  mHz. The wave packet propagates Earth-ward with group velocity about 10 km/s (close to the local plasma drift velocity) (Fig. 1). The behaviour of the magnetic field perturbations during this time interval is shown in Fig. 3. Time-frequency dependence of the ratio of  $VS(f)/|\mathbf{X}(f)|$  for the time interval 8:00-11:00 10/23/96 is shown in Fig. 2. The maximum at frequency about 2 mHz at 9:15–9:35 reaches 0.92. This indicates the existence of rotation of the

magnetic field vector. Vector makes a complete rotation during about 450 seconds, which corresponds to 2.22 mHz.

The spatial orientation of the plane of the magnetic field and the plasma flow vectors rotation is processed by use of the minimum variance analysis technique for vectors of the plasma velocity and the magnetic field perturbations. For the group of vectors  $\mathbf{A}_i = \{x_i, y_i, z_i\}$ ,  $i = 1, N$  the ratio of the eigen-values of the correlation matrix  $C_{ij}$  is investigated. Elements of  $C_{ij}$  are listed below:

$$\begin{aligned} C_{11} &= \sum x_i^2, & C_{12} &= \sum x_i y_i, & C_{13} &= \sum x_i z_i, \\ C_{21} &= \sum y_i x_i, & C_{22} &= \sum y_i^2, & C_{23} &= \sum y_i z_i, \\ C_{31} &= \sum z_i x_i, & C_{32} &= \sum z_i y_i, & C_{33} &= \sum z_i^2. \end{aligned} \quad (1)$$

One can use the dependence of the eigenvalues  $\lambda_1 > \lambda_2 > \lambda_3$  ratio to study the existence of some predominate direction in the processed vector group. If  $\lambda_1 \gg \lambda_2, \lambda_2$  and  $\lambda_3$  are of the same order of magnitude than there is the plane, which normal is estimated corresponding to the  $\lambda_3$  eigenvector. If  $\lambda_1$  and  $\lambda_2$  are of the same order of magnitude,  $\lambda_2 \gg \lambda_3$  the vectors in the group are randomly oriented. Application of the method of minimum variation to the processed vortex event determined the orientation of the plane of the vortex motion with the normal close to the direction of the background magnetic field. The observed structure can be determined as the vortex of the Alfvén type [23]. During the registration of vortex events the Poynting flux along the background magnetic field increases. The Poynting flux is taken in the approximation of ideal MHD [20]:

$$\mathbf{P} = 2\nu(\mathbf{B}_0 \cdot \mathbf{b}) - \mathbf{B}_0(\nu \cdot \mathbf{b}) - \mathbf{b}(\nu \cdot \mathbf{B}_0), \quad (2)$$

where  $\nu$  is the velocity of thermal plasma flow;  $\mathbf{B}_0$  and  $\mathbf{b}$  is the unperturbed and perturbed magnetic field, respectively. The absolute value of the Poynting vector increases up to 1–2 orders of magnitude in the vortex structure with predominate direction along the background magnetic field. The transverse velocity of the ULF wave packet for processed interval was estimated in [1] making use of the coordinated Inteball-Tail and ground based magnetic field measurements from CANOPUS magnetometer array. The group velocity of the wave packet was estimated to be 4–16 km/s (close to the plasma drift velocity). Assuming the velocity of vortex structure transverse to the background magnetic field to be close to the wave packet group velocity the transverse dimensions of the vortex structures is estimated to be about 1200–3600 km, that corresponds to several ion Larmor radii. It is significantly less than the spatial scales of vortex structure observed near the magnetopause [11, 12]. The observed velocity of the vortex structure is also much less than the usual velocity of the vortices generated by the Kelvin-Helmholtz instability, which is of the same order with the velocity of the magnetosheath plasma flow. Thus the

observed vortex structure is generated not by boundary flow instabilities and can be considered as the nonlinear phase of the high amplitude ULF waves. These structures can be processed as the stable solutions of the non-linear Hasegawa-Mima equation (with vector non-linearity: see [19] for details) that can be used as planar approximation of the Earth plasma sheet system with plasma density inhomogeneity transverse to the background magnetic field.

For the numerical simulation of vortex structures we provide the numerical scheme to study the two-dimensional perturbations dynamics in a frame of the Hasegawa-Mima equation. The numerical conservative scheme proposed in [6] with the Laplace-like equation solution technique based on full reduction algorithm (see details in [19]) was applied for numerical solution of this equation. The velocity of the vortex structure motion from numerical simulation is close to the local plasma drift velocity that confirms our approximation. The monopole structures are found to be stable. Slow dissipation is observed during 4–8 full rotations. The initial conditions in the form of three single monopole vortices with positive potential with different transverse size (from 2 to 6 ion Larmor radii) and the same amplitude are shown in Fig. 4. All the vortices demonstrate stable behaviour along trace length which is more than 10 times longer than the vortex initial scale.

## DISCUSSIONS AND CONCLUSIONS

The technique based on minimum variance analysis of magnetic field perturbation and its scalar and vector spectrum processing is extended to detect the vortex-like structures in magnetic field data. The proposed technique is applied to Inteball-Tail FGM data and the case study of vortex like structure propagating Earth-ward in the distant plasma sheath is presented. The observed event is associated with intense magnetic field perturbation during the recovery phase of the intermediate geomagnetic storm. The spatial scale of the vortex was found to be about 1200–3600 km (the spatial scale of the ULF packet was estimated to be about 1–3  $R_E$ ). The vortex polarization plane was found to be close to perpendicular to the background magnetic field and significant increase of the Poynting flux along the background magnetic field was observed. The vortex velocity transverse to the background magnetic field was of the same order with the local plasma drift velocity (about 10 km/s). The observed properties were confirmed by the numerical simulation of Alfvén like vortex in the inhomogeneous plasma: vortex with initial spatial scale about Larmor radius is stable enough to cover distance greater than 10 vortex scales, velocity was found to be about 0.5 of the  $V_d$ .

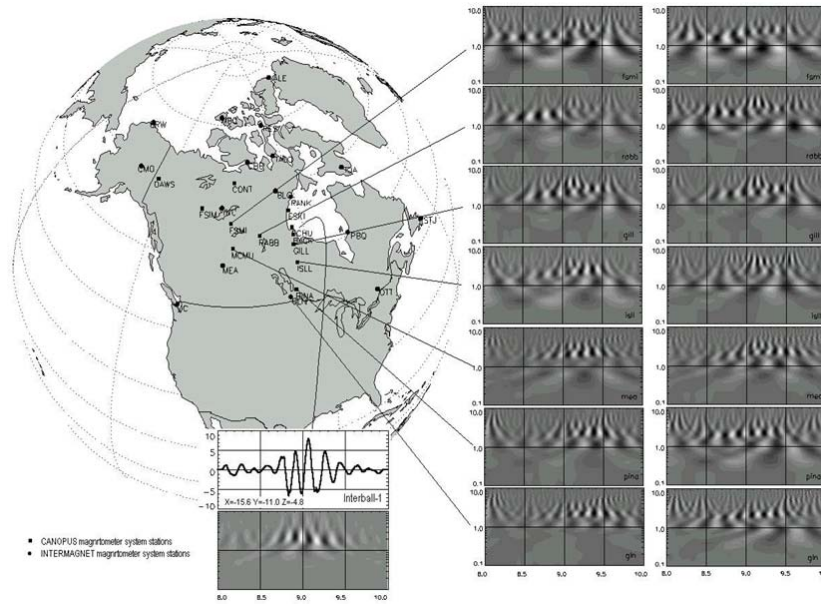


Fig. 1: The dynamics of Ps6 wave packet from magnetic field measurements provided by CANOPUS magnetometer stations. The real part of wavelet transform (Morlet) indicates well the localized in time (duration is about 1 hour) periodic process with frequency  $\sim 2$  mHz. The wave packet propagates Earth-ward with group velocity about 10 km/s (close to the local plasma drift velocity).

ACKNOWLEDGEMENT

Authors thank Yu. Yermolaev for CORALL data, M. Nozdrachev for MIF-M magnetometer data and CDAweb service for providing Inteball Tail dataset.

REFERENCES

[1] Agapitov O. 2004, Space Science and Technology, 5/6, 5  
 [2] Agapitov O. & Cheremnykh O. 2008, Ukr. Phys. J., 53, 5  
 [3] Agapitov A. V. & Cheremnykh O. K. 2011, Kinematika i Fizika Nebesnykh Tel, 27, 3, 17  
 [4] Agapitov A. V., Cheremnykh O. K. & Parnowski A. S. 2008, Adv. Space Res., 41, 1682  
 [5] Agapitov O., Glassmeier K.-H., Plaschke F. et al. 2009, J. Geophys. Res., 114, A00C27  
 [6] Arakawa A. 1997, Journal of Computational Physics, 135, 103  
 [7] Birn J., Hones E. W., Jr., Bame S. J. & Russell C. T. 1985, J. Geophys. Res., 90, 7449  
 [8] Connors M., Rostoker G., Sofko G., McPherron R. L. & Henderson M. G. 2003, Ann. Geophys., 21, 493  
 [9] Fairfield D. H., Otto A., Mukai T. et al. 2000, Geophys. Res., 105, 21159  
 [10] Hasegawa H., Fujimoto M., Phan T.-D. et al. 2004, Nature, 430, 755  
 [11] Hones E. W., Jr., Birn J., Bame S. J. et al. 1981, J. Geophys. Res., 86, 814  
 [12] Hones E. W., Jr., Birn J., Bame S. J. & Russell C. T. 1983, Geophys. Res. Lett., 10, 674  
 [13] Hones E. W., Paschmann G., Bame S. J. et al. 1978, GRL, 5, 1059  
 [14] Keiling A., Angelopoulos V., Runov A. et al. 2009, J. Geophys. Res., 114, A00C22  
 [15] Klimov S., Romanov S., Amata E. et al. 1997, Ann. Geophys., 15, 514  
 [16] Masters A., Achilleos N., Kivelson M. G. et al. 2010, J. Geophys. Res., 115, A07225  
 [17] Ohtani S., Rostoker G., Takahashi K. et al. 1999, J. Geophys. Res., 1999, 104, 2381  
 [18] Romanov S. A. 1998, Cosmic Research, 36, 317  
 [19] Saliuk D. & Agapitov O. 2011, Advances in Astronomy and Space Physics, 1, 69  
 [20] Saunders M. A., Southwood D. J., Hones E. W., Jr. & Russell C. T. 1981, J. Atmos. Terr. Phys., 43, 927  
 [21] Tang C. L. 2012, Ann. Geophys., 30, 537  
 [22] Verkhoglyadova O., Agapitov A., Andrushchenko A. et al. 1999, Ann. Geophys., 17, 1145  
 [23] Verkhoglyadova O. P., Agapitov A. V. & Ivchenko V. N. 2001, Adv. Space Res., 28, 801  
 [24] Yermolaev Yu. I., Fedorov A. O., Vaisberg, O. L. et al. 1997, Ann. Geophys., 15, 533  
 [25] Zong Q.-G., Wang Y. F., Yang B. et al. 2009, J. Geophys. Res., 114, A10211

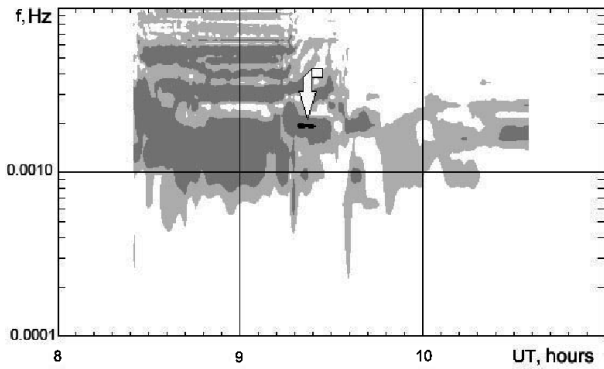


Fig. 2: The ratio of the modulus of the spectral density of the vector magnetic field perturbation spectrum to the total spectral density. The arrow indicates the presence of rotational oscillations.

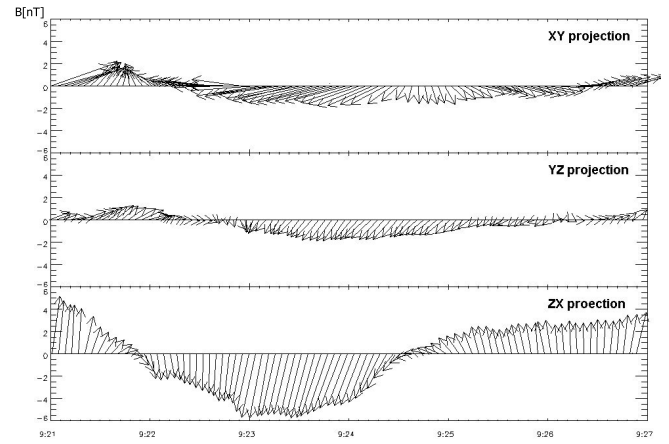


Fig. 3: Components of the vector magnetic field perturbation in the coordinate plane of coordinate system GSE 9:21-9:27 UT, 23.10.96.

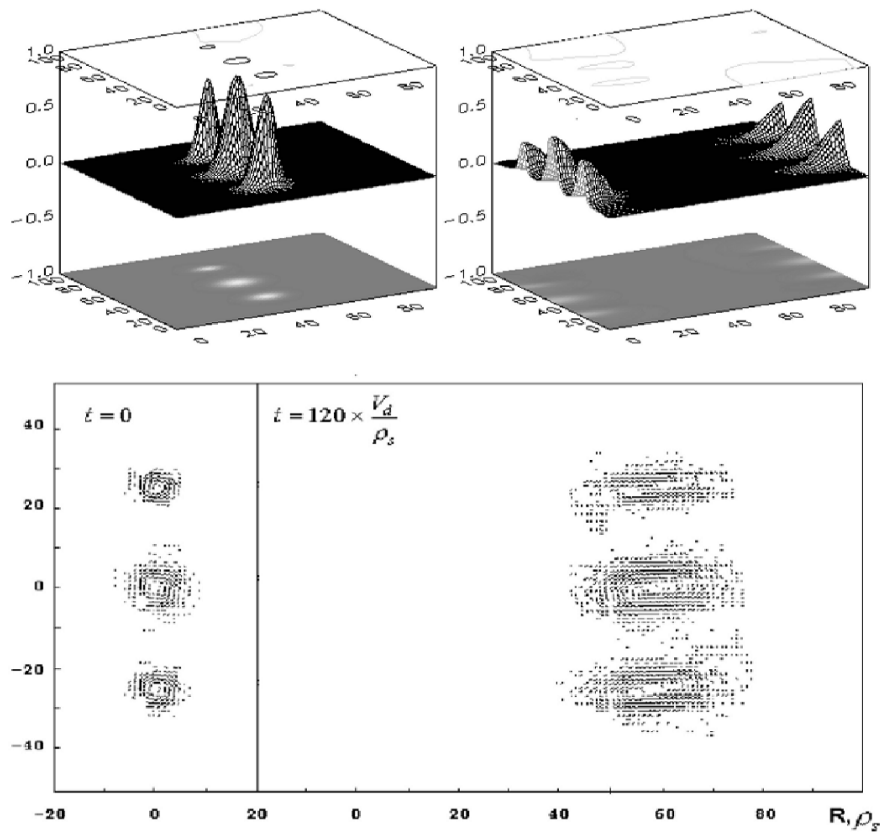


Fig. 4: The initial conditions in the form of three single monopole vortices with positive potential. At the beginning vortices have different transverse size and the same amplitude. After some time, the transverse dimensions of the vortices are aligned, the amplitudes are different, then they equally slow decay.